Int. J. Electrochem. Sci., 14 **(2019)** 8931 – 8938, doi: 10.20964/2019.09.45

International Journal of ELECTROCHEMICAL SCIENCE
www.electrochemsci.org

Short Communication

Highly Proton-conducting Hybrid Materials containing Keggin-type Tungstovanadophosphoric Acids and Organic Polymers

Wenshuang Dai[1], *Xia Tong*[2], *Qingyin Wu*[1,2,*]

[1] School of Biomedical and Chemical Engineering, Liaoning Institute of Science and Technology, Benxi 117004, Liaoning, P. R. China
[2] Department of Chemistry, Zhejiang University, Hangzhou, 310027, P. R. China
[*]E-mail: qywu@zju.edu.cn

Received: 3 May 2019 / *Accepted:* 2 July 2019 / *Published:* 31 July 2019

Four new proton-conducting hybrid materials were prepared by Keggin-type tungstovanadophosphoric heteropoly acids $H_4PW_{11}VO_{40}\cdot nH_2O$ ($PW_{11}V$) and $H_6PW_9V_3O_{40}\cdot nH_2O$ (PW_9V_3), organic polymers (polyvinylpyrrolidone, PVP or polyethylene glycol, PEG) and silica gel (SiO_2) at weight ratio of 80:10:10. Structural analysis reveals that the Keggin anions maintained in the hybrid materials, and these products exhibit high proton conductivity with 1.36×10^{-3} ($PVP/PW_{11}V/SiO_2$), 3.44×10^{-3} ($PEG/PW_{11}V/SiO_2$), 8.90×10^{-3} ($PVP/PW_9V_3/SiO_2$) and 1.63×10^{-2} $S\cdot cm^{-1}$ ($PEG/PW_9V_3/SiO_2$) at 26 °C and 75% relative humidity, increasing with higher temperature. Their activation energy of proton conduction is 17.96, 15.34, 17.54, 14.23 $kJ\cdot mol^{-1}$, respectively, which is lower than the corresponding pure acid. The proton conduction mechanisms of these materials are also proposed.

Keywords: Keggin structure; heteropoly acids; proton conductivity; hybrid materials; polyoxometalates.

1. INTRODUCTION

Heteropoly acids (HPAs) and their polyoxometalate salts (POMs), an increasingly significant class of inorganic metal oxo cluster compounds, have attracted much attentions in the past decades [1-7]. Due to their strong Brønsted acidity, HPAs can be served as highly efficient acid catalysts and their main application lies in the field of catalysis [8-11]. Recently, much effort has been made to the development of solid-state materials with proton conductivity because of their wide potential applications in electrochemistry. HPAs are widely known to perform high proton conductivity as their oxygen groups on the surface are able to bind water molecules [12-15]. Thus, they are excellent low-cost solid proton conductors and several papers have reported their applications in fuel cells [16, 17] or electrochemical capacitors [18, 19].

However, despite the good conductive performance of HPAs, their stability of electrochemical property is not desirable. Their proton conductivity can be strongly influenced by the relative humidity (RH) and ambient temperature, therefore limiting their broader applications. To overcome these drawbacks, as well as to improve flexibility and moldability of the materials, various attempts have been made to mix HPAs with organic polymers [20-23]. In these hybrid materials, HPAs dispersed uniformly in the polymers while their structures are still maintained, resulting in excellent chemical properties.

Silica gel, as an inorganic matric, can also be involved in the sol–gel process for the preparation of these inorganic-organic materials [24, 25]. HPAs can catalyze the hydrolysis of tetraethoxysilane (TEOS), the precursor for silica formation, and the presence of SiO_2 can improve the thermal stability and water retention properties of the composites. Besides, although the proton adsorption rate on ≡Si-OH surface is low under a normal pH range, HPA molecules with high acidity can increase the proton adsorption rate significantly, as well as the zeta potential and the number of positively charged $\equiv SiOH_2^+$ external groups [26].

Our group has reported a proton-conductive composite materials containing Keggin-type heteropoly acids and organic polymers [27]. In this study, we added silica gel in the preparation process to get four different hybrid materials. Their conductivity and proton conduction mechanisms have also been investigated and discussed.

2. EXPERIMENTAL SECTION

2.1 Preparation of ternary hybrid materials

$H_4PW_{11}VO_{40}\cdot nH_2O$ ($PW_{11}V$) and $H_6PW_9V_3O_{40}\cdot nH_2O$ (PW_9V_3) were synthesized according to our previous papers [27, 28]. Four ternary hybrid materials were obtained by the following procedures: 3.2g of HPA ($PW_{11}V$ or PW_9V_3) was dissolved in 20mL of hot water, combined with 1.12 mL of tetraethoxysilane (TEOS), and stirred for 3 h at room temperature. 20 mL of organic polymer (polyvinylpyrrolidone, PVP, MW=38000 or polyethylene glycol, PEG, MW=20000) solution was added dropwise into the mixture, with the weight ratio of HPA: SiO_2: organic polymer equals to 80:10:10, and kept stirring for another 12 h. The mixed solution was then put into the oven at 50 °C, dried and crushed to powdery product.

2.2 Instruments and reagents

FTIR spectra were recorded on a NICOLET NEXUS 470 FT/IR spectrometer over the wavenumber range 400-4000 cm^{-1} using KBr pellets, with the resolution of 4 cm^{-1}. X-ray powder diffraction (XRD) patterns were obtained with a BRUKER D8 ADVANCE X-ray diffractometer using a Cu tube operated at 40 kV and 40 mA in the range of 2θ=5-40° at a rate of $0.02°\cdot s^{-1}$. The electrochemical impedance measurement was performed on a VMP2 Multichannel potentiostat electrochemical impedance analyzer over a frequency range from 9.99×10^4 to 0.01 Hz. The hybrid materials were compressed to pellets with 10mm diameter under 20 MPa pressure at room temperature

(26 °C) and 75% relative humidity (RH). The thicknesses for different samples were 2.77 mm ($PVP/PW_{11}V/SiO_2$), 2.02 mm ($PEG/PW_{11}V/SiO_2$), 3.04 mm ($PVP/PW_9V_3/SiO_2$) and 2.97 mm ($PEG/PW_9V_3/SiO_2$), respectively. The proton conductivity was measured by using a cell: Cu|sample|Cu, with pellets sandwiched by two copper sheets. Copper electrodes and wires were applied in these measurements.

All reagents were of analytical grade.

3. RESULTS AND DISCUSSION

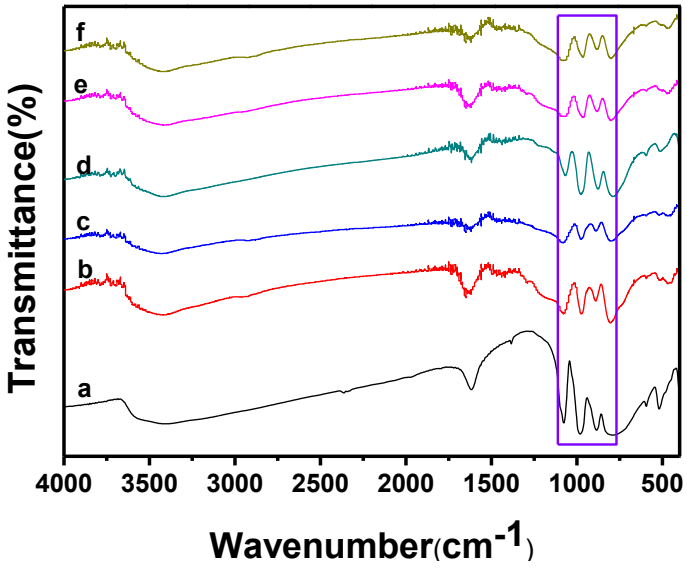

Figure 1. IR spectra of (a) $PW_{11}V$, (b) $PVP/PW_{11}V/SiO_2$, (c) $PEG/PW_{11}V/SiO_2$, (d) PW_9V_3, (e) $PVP/PW_9V_3/SiO_2$, (f) $PEG/PW_9V_3/SiO_2$.

IR spectroscopy is helpful to define the composition and structure of hybrid materials. Fig. 1 presents the IR spectra of the synthesized products and their corresponding pure heteropoly acid. Generally, Keggin-type HPA shows characteristic peaks at 700-1100 cm^{-1}. All samples contain four characteristic bands at that fingerprint region, including about 1080, 970, 890, 805 cm^{-1}, assigned to the stretching modes of P–O_a, terminal M-O_d, edge sharing M-O_b-M and corner-sharing M-O_c-M units (M=W,V), respectively. Although the heteropoly anions maintain their Keggin structures in these materials, several frequency shifts occurred in those peaks when compared to each other, which can be attributed to the interactions among HPAs, SiO_2 and different organic polymers. As M-O_b-M and M-O_c-M vibrations may involve some bending character, the competition of the opposite effects exists, namely, the weakness of electrostatic anion−anion interactions leads to a decrease in the stretching frequencies and an increase in the bending frequencies, suggesting opposite frequency shifts directions between M-O_b-M and M-O_c-M. This is convinced by the red shift of M-O_b-M from 890 cm^{-1} ($PW_{11}V$) to 888 cm^{-1} ($PVP/PW_{11}V/SiO_2$ and $PEG/PW_{11}V/SiO_2$), 883cm^{-1} (PW_9V_3) to 878 cm^{-1}($PVP/PW_9V_3/SiO_2$) and 879cm^{-1} ($PEG/PW_9V_3/SiO_2$) and the blue shift of M-O_c-M from 795 cm^{-1} ($PW_{11}V$) to 807 cm^{-1}

(PVP/$PW_{11}V/SiO_2$ and PEG/$PW_{11}V/SiO_2$), 790cm^{-1} (PW_9V_3) to 805 cm^{-1} (PVP/PW_9V_3/SiO_2) and 804 cm^{-1} (PEG/PW_9V_3/SiO_2).

In the spectra of hybrid materials, the peak of SiO_2 can be observed at approximately 450 cm^{-1}, which is assigned to the ring structure of SiO_4 bending vibration. A wide peak at approximately 1080 cm^{-1} is due to the overlap between the Si-O-Si stretching vibration peak and the P–O band. Due to the presence of PEG or PVP polymer, characteristic bands of C-H vibration can be observed. Peaks at approximately 1290~1300cm^{-1} and 2920~2930cm^{-1} are attributed to C-H bending vibration and stretching vibration, respectively. In addition, a broad band in the high wavenumber region 2990–3600cm^{-1} can be observed in all the curves, which arises from the O-H stretching of water molecules. Compared to curve a and d, the bands attribute to O-H stretching bands becomes broader and exhibits a bit blue shifts, indicating a large number of hydrogen bonds between HPAs, SiO_2 and polymers are formed and their interactions increased.

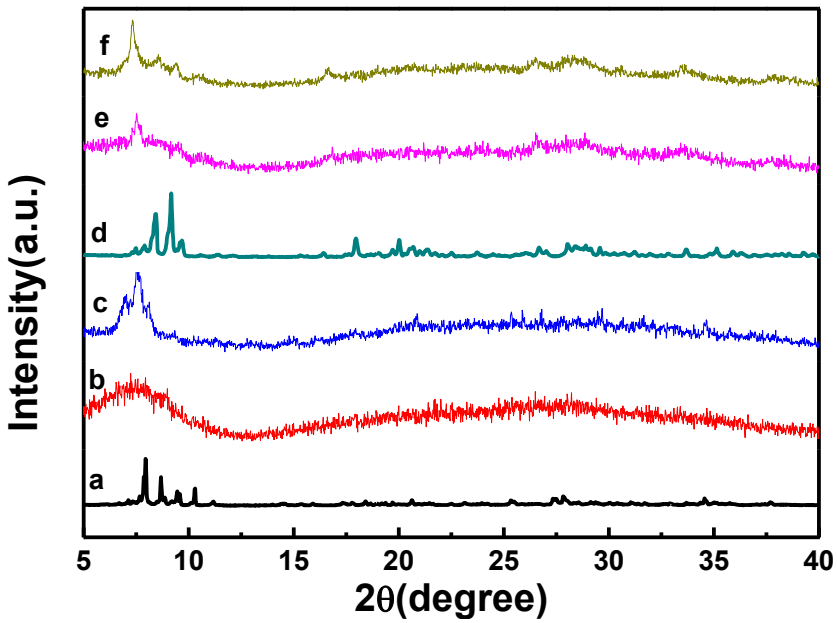

Figure 2. XRD patterns of (a) $PW_{11}V$, (b) PVP/$PW_{11}V/SiO_2$, (c) PEG/$PW_{11}V/SiO_2$, (d) PW_9V_3, (e) PVP/PW_9V_3/SiO_2, (f) PEG/PW_9V_3/SiO_2

X-ray diffraction (XRD) patterns of hybrid materials are presented in Fig. 2. Although the intensities varied because of the addition of PVP/PEG and SiO_2, characteristic peaks that attributed to Keggin structures still appeared at about 6-10° in curve b, c, e and f, which indicates the existence of Keggin-type anions in the materials, and is in agreement with the result from IR analysis. In curve a and d, certain sharp peaks indicate that $PW_{11}V$ and PW_9V_3 have high crystallinity. While the broad peaks at 15-38° suggest that these samples are amorphous without long-range order [29].

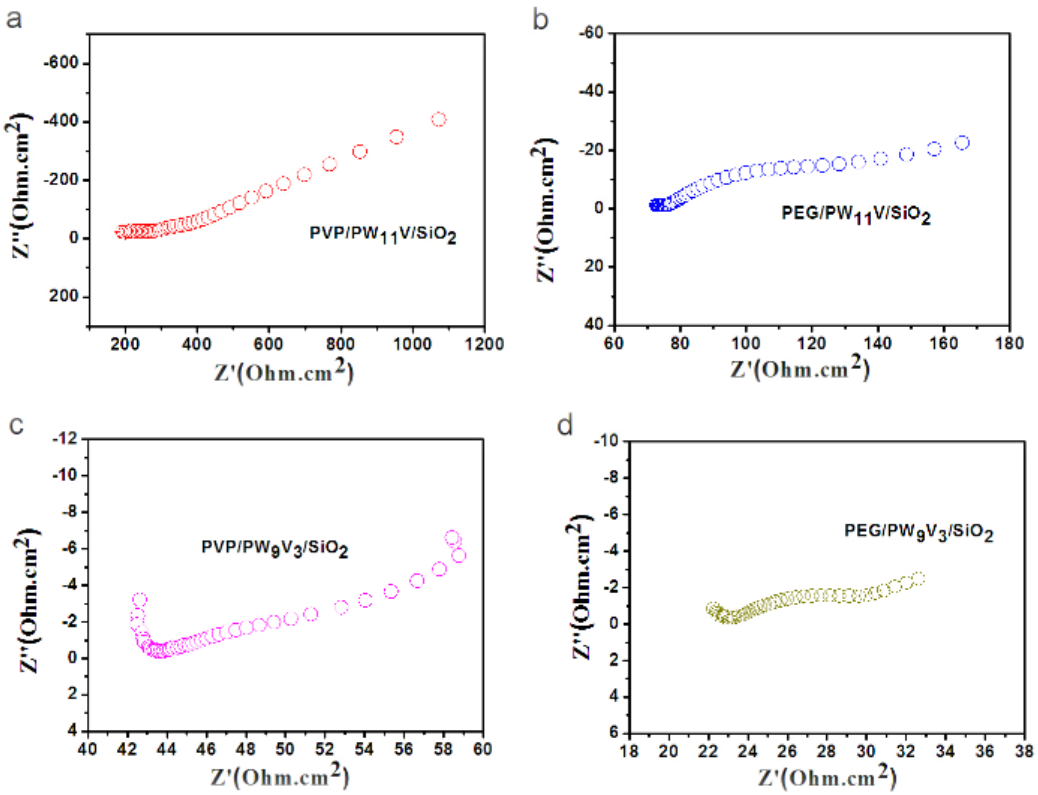

Figure 3. EIS of (a) PVP/$PW_{11}V/SiO_2$, (b) PEG/$PW_{11}V/SiO_2$, (c) PVP/PW_9V_3/SiO_2, (d) PEG/PW_9V_3/SiO_2 at 26°C and 75% relative humidity (RH).

Proton conductivity was evaluated by electrochemical impedance spectroscopy (EIS) analysis (Fig.3). It can be calculated with formula $\sigma = (1/R) \bullet (h/S)$, where h is the thickness and S is the surface area of the pellet. R is the resistance, which can be obtained from the EIS diagram. Therefore, the conductivity of PVP/$PW_{11}V/SiO_2$, PEG/$PW_{11}V/SiO_2$ is calculated as 1.36×10^{-3} and 3.44×10^{-3} $S\cdot cm^{-1}$, while that of PVP/PW_9V_3/SiO_2, PEG/PW_9V_3/SiO_2 is 8.90×10^{-3} and 1.63×10^{-2} $S\cdot cm^{-1}$, respectively. It is obvious that the material with more vanadium and the PEG-containing material has higher proton conductivity than its counterpart. It can be explained as the PEG is more favorable than PVP for the formation of hydrogen bonds. In addition, the introduction of SiO_2 also tends to form more hydrogen bonds and make the proton conduction much faster.

Conductivity reflects proton movement, and the Vehicle mechanism [30] and the Grotthuss mechanism [31] are the two prevalent mechanisms for proton conduction. In general, the activation energy of the Vehicle mechanism is relatively higher (20 kJ/mol or more), when compared to that of the Grotthuss mechanism (10 kJ/mol or less) [32, 33].

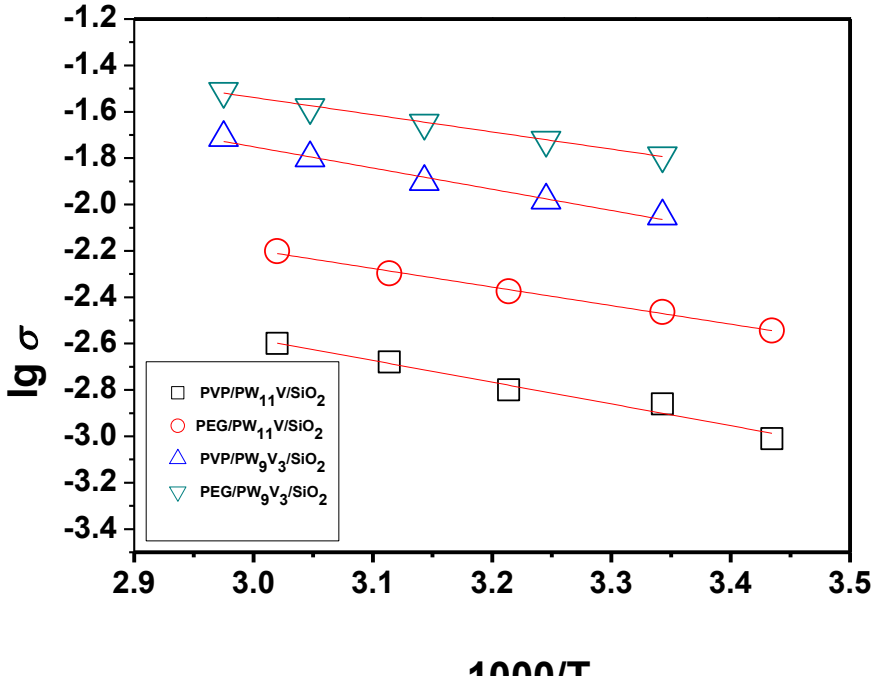

Figure 4. Arrhenius plots of proton conductivity of the hybrid materials.

Fig. 4 presents Arrhenius plots of the proton conductivity as a function of temperature for all the materials. It is obvious from this figure that the proton conductivity increased with increasing temperature. The activation energy (E_α) of conductivity can be calculated from the slope by using the equation $\sigma=\sigma_0 \exp(E_\alpha/\kappa T)$, where σ_0 is the preexponential factor and κ is the Boltzmann constant.

Table 1. Activation energy of proton conduction of the hybrid materials

Sample	Activation energy / kJ·mol^{-1}
$PW_{11}V$	25.66
$PVP/PW_{11}V/SiO_2$	17.96
$PEG/PW_{11}V/SiO_2$	15.34
PW_9V_3	25.68
$PVP/PW_9V_3/SiO_2$	17.54
$PEG/PW_9V_3/SiO_2$	14.23

The activation energy of all the materials is listed in Table 1. In the hybrid materials, HPAs, organic polymers and SiO_2 form a hydrogen-bonded network, through which protons can transport much easier, leading to lower activation energies. Also, the calculating results allow us to conclude that proton conduction in these materials is based on a mixed mechanism, in which Grotthuss mechanism is more predominant than Vehicle mechanism. The schematic illustration of this mixed mechanism (using $PVP/PW_{11}V/SiO_2$ as an example) is shown in Fig.5.

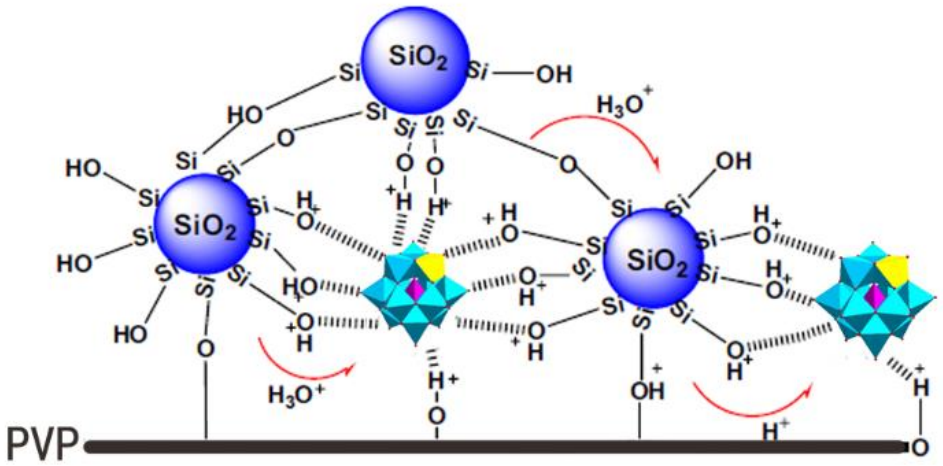

Figure 5. Schematic illustration of proton conduction in the PVP/$PW_{11}V/SiO_2$.

4. CONCLUSIONS

Highly proton-conducting hybrid materials: PVP/$PW_{11}V/SiO_2$, PEG/$PW_{11}V/SiO_2$, PVP/PW_9V_3/SiO_2 and PEG/$PW_{11}V/SiO_2$ were prepared by sol-gel methods. In all of these materials, HPAs maintain their Keggin structures, while the interactions with organic polymers (PVP or PEG) and SiO_2 also exist according to the structural analysis on IR and XRD results. Their proton conductivity is up to 10^{-3} $S \cdot cm^{-1}$ at 26 °C and 75% relative humidity. Their activation energy of proton conduction is between 10kJ/mol and 20kJ/mol, indicating mixed proton conduction mechanisms, in which Grotthuss mechanism is more predominant than Vehicle mechanism. The high conductivity and low activation energy of proton conduction of these hybrid materials makes them promising proton-conducting solid electrolytes for applications.

ACKNOWLEDGEMENTS
This work is financially supported by the Zhejiang Provincial Natural Science Foundation of China (LY18B010001), the Liaoning Provincial Natural Science Foundation of China (201602404) and the Foundation of Liaoning Educational Committee (L201710311).

References

1. M. Shiddiq, D. Komijani, Y. Duan, A. Gaita-Ariño, E. Coronado and S. Hill, *Nature*, 531 (2016) 348.
2. O. Sadeghi, L. N. Zakharov and M. Nyman, *Science*, 347 (2015) 1359.
3. X. Meng, H. N. Wang, S. Y. Song and H. J. Zhang, *Chem. Soc. Rev.*, 46 (2017) 480.
4. V. A. Kolesov, C. Fuentes-Hernandez, W. F. Chou, N. Aizawa, F. A. Larrain, M. Wang, A. Perrotta, S. Choi, S. Graham, G. C. Bazan, T. Q. Nguyen, S. R. Marder and B. Kippelen, *Nat. Mater.*, 16 (2017) 474.

5. J. J. Chen, M. D. Symes, S. C. Fan, M. S. Zheng, H. N. Miras, Q. F. Dong and L. Cronin, *Adv. Mater.*, 27 (2017) 4649.
6. M. Bonchio, Z. Syrgiannis, M. Burian, N. Marino, E. Pizzolato, K. Dirian, F. Rigodanza, G. A. Volpato, G. La Ganga, N. Demitri, S. Berardi, H. Amenitsch, D. M.Guldi, S. Caramori, C. A. Bignozzi, A. Sartorel and M. Prato, *Nat. Chem.*, 11 (2019) 146.
7. J. Miao, Z. L. Lang, X. Y. Zhang, W. G. Kong, O. W. Peng, Y. Yang, S. P. Wang, J. J. Cheng, T. C. He, A. Amini, Q. Y. Wu, Z. P. Zheng, Z. K.Tang and C. Cheng, *Adv. Funct. Mater.*, 29 (2019) 1805893.
8. J. Albert, D. Lüders, A. Bösmann, D. M. Guldi and P. Wasserscheid, *Green Chem.*, 16 (2014) 226.
9. R. Dutta, S. K. Singh, S. A. Mandavgane and J. D. Ekhe, *Appl. Catal. A.*, 539 (2017) 38.
10. L.M.Ai, D. F. Zhang, Q. Wang, J. S. Yan and Q. Y. Wu, *Catal. Commun.*, 126 (2019) 10.
11. J.S. Yan, Z. Q. Wang, Y. S. E, F. W. He, D. F. Zhang and Q.Y. Wu, *RSC Adv.*, 9 (2019) 8404.
12. G. Lakshminarayana and M. Nogami, *Electrochim. Acta*, 54 (2009) 4731.
13. X. F. Wu, T. P. Huang, Q. Y. Wu and L. Xu, *Dalton Trans.*, 45 (2016) 271.
14. Z. R. Xie, H.Wu, Q.Y. Wu and L. M. Ai, *RSC Adv.*, 8 (2018) 13984.
15. Z. R. Xie, Q. Y. Wu, F. W. He and L. M. Ai, *Funct. Mater. Lett.*, 11 (2018) 1850065.
16. S. Y. Oh, T. Yoshida, G. Kawamura, H. Muto, M. Sakai and A. Matsuda, *J. Mater. Chem.*, 20 (2010) 6359.
17. H. Wu, X. F. Wu, Q.Y. Wu and W. F. Yan, *Compos. Sci. Technol.*, 162 (2018) 1.
18. H. Gao and K. Lian, *J. Mater. Chem. A*, 4 (2016) 9585.
19. Z. R. Xie, Q. Y. Wu, W. S. Dai and F. W. He, *Int. J. Electrochem. Sci.*, 13 (2018) 11684.
20. M. B. McDonald and M. S. Freund, *ACS Appl. Mater. Interfaces*, 3 (2011) 1003.
21. U. Thanganathan and M. Nogami, *J. Solid State Electrochem.*, 18 (2014) 97.
22. N. Q. Tian, X. F. Wu, B. H. Yang, Q. Y. Wu, F. H. Cao, W. F. Yan and A. B. Yaroslavtsev, *J. Appl. Polym. Sci.*, 132 (2015) 42204.
23. H. Wu, H. X. Cai, Y. R. Xu, Q. Y. Wu and W. F. Yan, *Mater. Chem. Phys.*, 215 (2018) 163.
24. M. Aparicio, Y. Castro and A. Duran, *Solid State Ionics*, 176 (2005) 333.
25. S. W. Wang, F. L. Dong and Z. F. Li, *J. Mater. Sci.*, 47 (2012) 4743.
26. A. Pettersson and J. B. Rosenholm, *Langmuir*, 18 (2002) 8447.
27. X. Tong, N. Q. Tian, W. Wu, W.M. Zhu, Q.Y. Wu, F.H. Cao, W.F. Yan and A. B. Yaroslavtsev, *J. Phys. Chem. C*, 117 (2013) 3258.
28. X. Tong, N. Q. Tian, W. M. Zhu, Q.Y. Wu, F. H. Cao and W. F. Yan, *J. Alloys Compd.*, 544 (2012) 37.
29. M. Nagai, K. Kobayashi and Y. Nakajima, *Solid State Ionics*, 136 (2000) 249.
30. K.D. Kreuer, W. Weppner and A. Rabenau, *Angew. Chem. Int. Ed.*, 21 (1982) 208.
31. N. Agmon, *Chem. Phys. Lett.*, 244 (1995) 456.
32. K. Cheückiewicz, G. Zúukowska and W. Wieczorek, *Chem. Mater.*, 13 (2001) 379.
33. Q. Y. Wu, X. Y. Qian and S. M. Zhou, *J. Xuzhou Inst. Tech. (Nat. Sci. Ed.)*, 27 (2012) 1.